

# EXPERIMENTAL STUDY OF THE IN-PLANE BEHAVIOUR OF RAMMED EARTH WALLS STRENGTHENED WITH TRM

Michiel Van Gorp, Els Verstrynge, KU Leuven  
Daniel Oliveira, Rui Silva, Antonio Romanazzi, UMinho

## Abstract

Among the building techniques based on the use of raw earth as building material, rammed earth is one of the most used construction materials across the world. Rammed earth structures are characterized by low resistance against extreme loading, such as during earthquakes. Basing on the efficacy of Textile Reinforced Mortar (TRM) for masonry structures, the use of low-cost mesh embedded in earth-based mortar is proposed as a strengthening technique for rammed earth heritage.

The base materials were characterized, namely soil, earth-based mortar and two type of mesh (nylon and glass fibre).

Subsequently, eight walls were cast using the characterized soil and reinforced with glass fibre TRM (GRE) and nylon TRM (NRE). To assess the efficacy of the TRM, diagonal compression tests were performed and the shear strength and shear stress were evaluated and compared with the unreinforced walls. Digital image correlation (DIC) was implemented to investigate the crack pattern.

The results demonstrate that TRM improves the shear performance of the rammed earth walls in terms of shear strength and shear strain.

**Keywords:** Rammed Earth, Textile Reinforced Mortar, Earth, Materials, Consolidation

## 1. Introduction

Raw earth as building material is used in large parts of the world. A study by Houben and Guillaud (1989) projects that 30% to 40% of the earth's population lives in houses made of earth (fig. 1).

Rammed earth, like cob and adobe, is a construction technique that makes use of raw earth. Indeed, the product is readily available, low-cost and very sustainable. But as with masonry, historical earthen constructions can be vulnerable to certain types of forces. For example, cyclic and vibration type forces, normally visible during earthquakes. This effect certainly has its role for rammed earth, as this material is mostly used in regions which are very earthquake sensitive. (fig. 1)

Rammed earth as a construction technique dates back to prehistoric China, where civilizations built rammed earth houses resembling caves, the first known "place of residence" of mankind (Jaquin, 2012). However, the first true example of rammed earth construction can be found during the Three Kingdoms Period (221-581 AD), where the Haka people built Tulou houses. Using long poles fixed or driven into the ground, they were the first to hold the formwork in its place (Aaberg-Jorgensen, 2000). Later on, large parts of the Great Wall of China would also be built using rammed earth, mostly in desolate places, where bricks were not readily available (Jaquin, Augarde and Gerrard, 2008).

The rammed earth technique consists of compacting layers of moistened soil within a formwork. The soil used for building should meet specific requirements to reduce the risk of shrinkage and to ensure suitable dry density. (Houben and Guillaud, (1989)).

Rammed earth as a construction material possesses many qualities that cannot be found in other materials. Earth is available on a local scale and in abundance, lowering cost of transportation. It has a low impact on the environment, reducing the CO<sub>2</sub> emissions of the building drastically (Morel et al., 2001). Other qualities include its ability to increase indoor air

quality (Pacheco-Torgal and Jalali, 2012), its ability to absorb moisture (Minke, 2000) and reusability (Venkatarama and Prasanna, 2010).



**Figure 1:** Remark the significant overlap between the regions, where rammed earth buildings are common (left), and the territories with a moderate to very high seismic hazard (right) (source: CRATerre)

Rammed earth structures are characterized by low compressive and tensile strength which combined with high self-weight of the material and lack of connection between structural elements, results in high vulnerability of the building (Bui, 2009) (Silva, 2013). This is certainly the case for historical constructions, as using additives to better the characteristics of the soil was not common practice. If a rammed earth wall contains too much clay, cracking due to shrinkage will result (Warren, 1999). The shrinkage behaviour cannot be avoided, but measures can be taken to minimize it. It is therefore imperative to avoid a higher water content than is absolutely necessary during compaction, as it will lead to higher shrinkage when drying. When cracks occur, a loss in compressive strength is found (Silva et al, 2013).

As demonstrated in case of masonry buildings, textile reinforced mortar (TRM) represents an effective strengthening solution because of its high tensile strength, low weight and high ductility. The TRM is a composite material that “increases the deformability of materials subjected to in-plane loading forces” (Papanicolau, 2007). It consists of a textile mesh embedded in mortar, applied to the surface of the original construction. In other words, TRM increases the load-bearing capacity of the structure, while at the same time homogenizing the structural response (Bernat-Maso, 2013).

The effectiveness of the TRM depends on the characteristics of the components and their compatibility with the substrate. Indeed, in case of rammed earth, too stiff and too strong materials require deformation levels which could cause the collapse of existing structures, thus resulting in an unsuccessful strengthening contribution. In the present instance, the mesh is required to be affordable as well (Oliveira et al., 2017). The most important qualities of the mesh are its tensile behaviour and deformation capability (De Santis and de Felice, 2014).

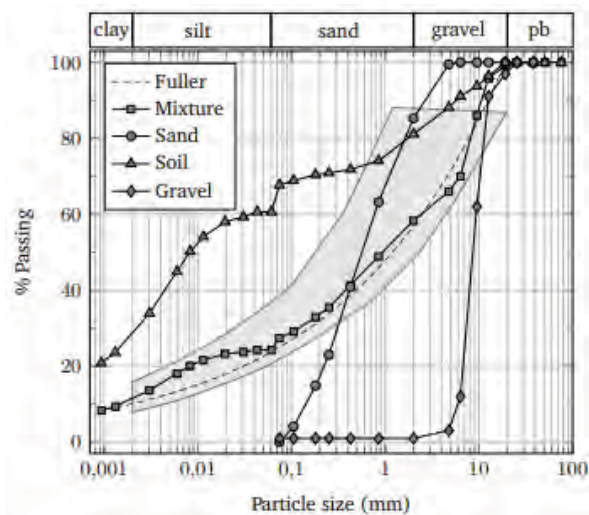
The effectiveness of TRM on rammed earth walls was investigated by means of diagonal compression tests. In general, two types of behaviour can be assessed when looking at real life earthen constructions damaged by for example earthquakes: flexural behaviour (failure mode: crushing or rocking) and shear behaviour (failure mode: diagonal shear cracking or sliding shear failure). In literature, simplified models are presented, focusing on one type of these behaviours. Assuming a model where a corner of the wall is loaded with an in-plane point load, the dominant behaviour of the model can be addressed to shear forces and a diagonal shear crack as its failure mode (Calderini et al., 2010). This model can be tested using the diagonal compression test, as described in the standard ASTM E 519 – 02 (ASTM, 2003). While the diagonal compression test has not been assessed for rammed earth strengthened with TRM previous to the writing of this work, test procedures and results for masonry structures can be used. Here, TRM is presented as a viable solution for the consolidation of masonry structures (Papanicolau et al., 2007).

## 2. Materials

Not every soil qualifies as a base material for rammed earth. It requires some clay as binding agent, but not too much to avoid shrinkage. It requires a good mixture of gravel, sand and silt to create a strong and dense stabilizing framework. Yet, dry density is only optimal within a small range of water content. To satisfy all these requirements, the soil is characterized and subsequently engineered. From this engineered soil, eight rammed earth walls are produced for the TRM tests.

A similar engineering effort is performed on the mortars. Workability is improved, yet its strength and mechanical compatibility to the rammed earth wall is retained as much as possible. Of the tested mortars, one is selected for the TRM-compositions.

**Earth.** The soil used for rammed earth walls and earth-based mortar was collected from a quarry at Amoreiras-Gare in Alentejo, South-Portugal. This is an area where rammed earth construction has been utilized for centuries. Fig. 2 shows the particle size distribution of the soil in comparison with recommendations found in literature (WB Fuller 1907, Houben and Guillaud 1989) which ensure reduced shrinkage and suitable dry density, and thus a suitable compressive strength. The results show high content of clay and silk and low presence of sand and gravel fraction.

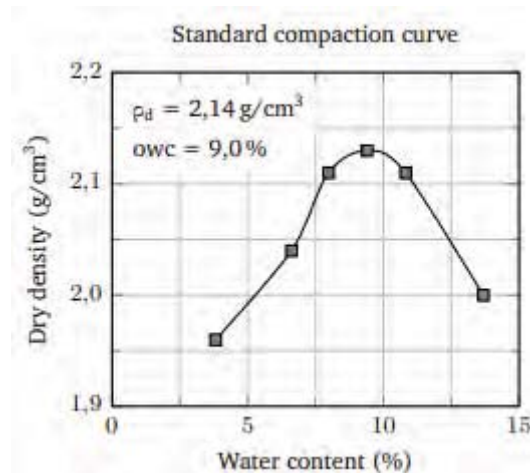


**Figur 2:** Particle size distribution of the original soil and the corrected mixture

To meet the requirements found in literature, the base soil is subsequently engineered by volume mixing 40% of the base soil with 35% sand and 25% gravel (Mixture in fig. 2).

Construction of rammed earth walls requires the use of earth with the right water content. Too much water in the “voids” prevents the earth from compacting during ramming. Too low a water content increases particle friction which leads to an insufficient compaction rate during the ramming process. The optimal water content was determined in the lab by means of the Proctor compaction test (LNEC E197). As the purpose is to investigate traditional rammed earth walls manually compacted, a manual Proctor test was conducted.

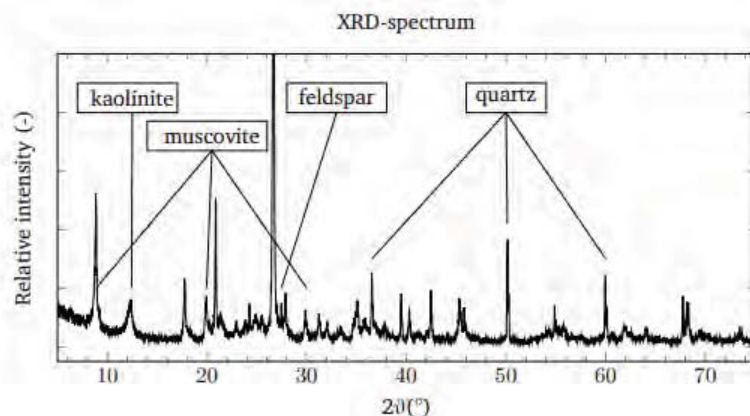
Six specimens were compacted with different water content and their dry density was assessed. The compaction curve of the measurements is shown in fig. 3. A range of dry density between 2,10 g/cm<sup>3</sup> and 2,20 g/cm<sup>3</sup> guarantees suitable compressive strength of rammed earth elements. The dry density of the soil mixture is 2,14 g/cm<sup>3</sup> for an optimal water content (OWC) of around 9%.



**Figuur 3:** Standard Proctor test according to LNEC E197 standard

Clay is vital to the strength and bonding of the mixture. However, swelling clays are known to induce cracks during drying. Rammed earth walls may lose their strength as a result. To investigate the type of clays in the mixture, an X-ray diffraction (XRD) analysis is carried out on the soil using a Philips PW-1830 diffractometer. The analysis (fig. 4) shows the presence of quartz, mica (muscovite and goethite), feldspar (potassium feldspar and plagioclase), hematite and some traces of chlorite. The presence of hematite and goethite is consistent with the red-brownish colour of the soil. None of the detected minerals are known as swelling clays (Velde, 2008). Only muscovite, which is related to the illite group of clays, shows mild expansion under wetting. The lack of expansive clays makes the appearance of cracks during the drying process of the rammed earth walls less probable.

A methylene blue test was used to validate the XRD results. With a clay activity index of 4.5 g/kg, the soil can be classified as a class 3 soil or “soil with a not very active clay fraction”, according to the classification of Lautrin (1989).



**Figuur 4:** XRD-spectrum of the fine grain fraction of the soil mixture

In summary, a soil mixture has been engineered that is suitable for the production of rammed earth walls. The particle size distribution is in line with recommendations and no major swelling clays are present. The compaction rate and optimal water content correspond to literature, reducing the risks of cracking and instability. Further tests on the consistency, specific gravity and mechanical characteristics confirm results set in literature (Van Gorp, 2018).

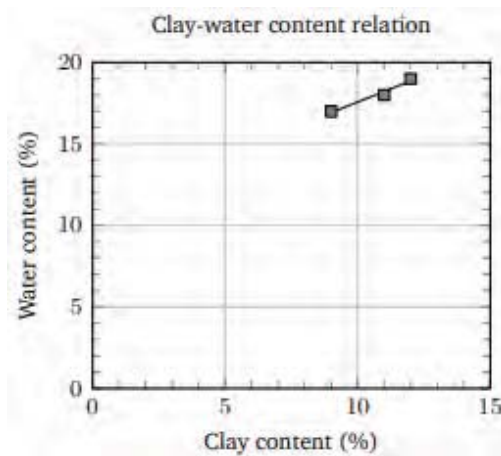
**Mortar.** A successful TRM mortar has the capacity to transfer stress between the wall and the textile. It is compatible with heritage rammed earth so that a strong adhesion is guaranteed, even in the case of retrofitting. Compatibility with heritage buildings implies the use of an

unsterilized earth mortar. No additives should be considered. So, only clay will be used as a binding agent. Stronger earth mortars typically have a higher clay content which increases the risk of drying cracks. The balance between strength and compatibility is essential in identifying a compatible mortar.

Three earth-based mortars were prepared using the same base soil as used for the rammed earth. However, only the material with a grain size smaller than 2 mm is considered here. Each mortar consists of a different ratio of soil and fine sand, to reduce the clay content of the mixture.

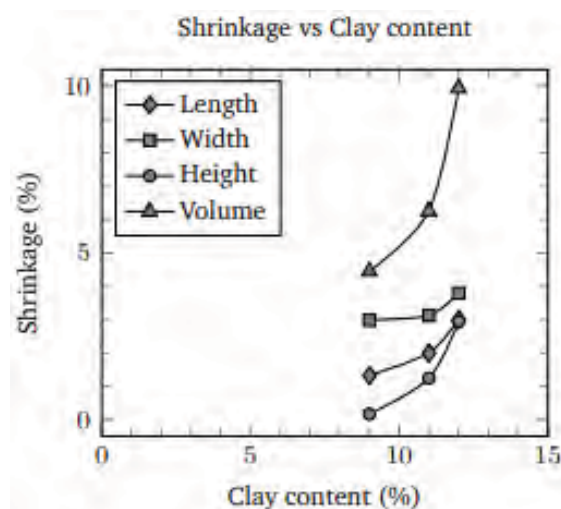
According to Gomes (2013), workability is controlled by adding water to the sand-soil mixture. It is prioritized over other parameters, as it is an indispensable quality of any mortar. The results can be found in fig. 5.

Mortars with a higher soil/sand ratio require a higher water content to reach optimal workability. Mortars with lower water content are preferred as they are less vulnerable to cracking as a result of shrinkage.



**Figuur 5:** Clay content vs water content for three mortars for optimal workability

The Alcock test was conducted to evaluate the linear shrinkage of mortar beams and results are depicted in fig. 6. Aside from the length, the volumetric shrinkage and shrinkage of the height and width are also measured. However, the results show immediately that the shrinkage of the length is not representative for the other dimensions. The mortar with the highest clay content was not considered for further testing, as its linear shrinkage levels do not meet the maximum linear shrinkage value of 2%, as suggested in literature by Gomes (2013).



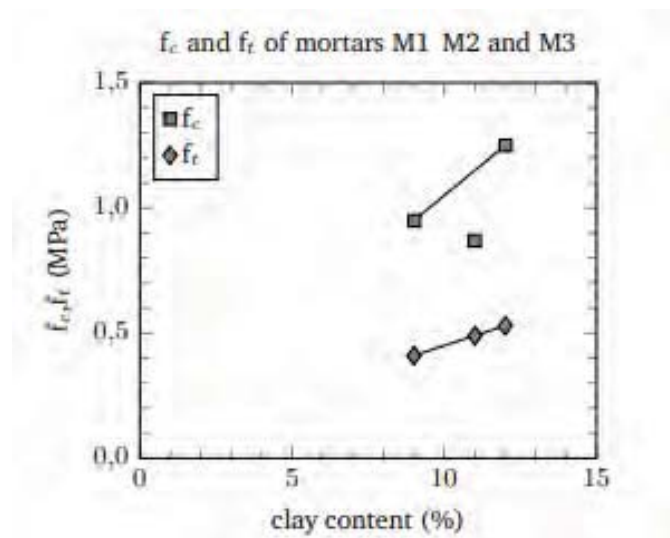
**Figuur 6:** Linear and volumetric shrinkage for several mortars



The shrinkage values show a dependency on the clay content. As expected, shrinkage is larger for mortars with a larger clay content. The effect is especially noticeable in the volumetric shrinkage. A change in clay content of 2% results in a doubling of the volumetric shrinkage.

Finally, the compressive ( $f_c$ ) and flexural strength ( $f_t$ ) of the mortar specimens were assessed according to the EN 1015-11 standard using a LLOYD instruments automatic press LR 50K Plus. Test results are reported in fig. 7. Both strengths increase with the clay content of the mortar. The mortar with the highest clay content presented the highest compressive strength, as expected. Similar results are found in Barroso (2017), where a direct correlation between compressive strength and clay content was observed. The flexural strength is about half of the compressive strength, which is in line with expectations.

In order to avoid premature cracking in the TRM, the mortar for strengthening was selected fixing a threshold of linear shrinkage of 2%, making mixture M1 the most sensible choice, while also presenting the most suitable mechanical strength.



**Figur 7:** Compressive strength ( $f_c$ ) and tensile strength ( $f_t$ ) values of mortars against clay content

### 3. Diagonal Compression Tests

Shear stress is an important component through which earthquakes damage walls. It therefore makes sense to investigate how new and existing rammed earth buildings can be improved to better withstand earthquakes. Previously, we explained how to engineer and test a soil mixture, suitable for the construction of rammed earth walls. Next to this, a mortar was tested, envisioning an improved protection of the walls when subjected to in-plane shear stress. In this chapter, these materials are used to build eight rammed earth walls. Three were reinforced with a glass-fibre based TRM (GRE), two with a nylon-based TRM (NRE), while three walls remained unreinforced (URE). The in-plane shear stress was generated as part of a diagonal compression test (ASTM E519-02, 2003). Measurement results were obtained through LVDT and control-unit readings. In addition, a digital image correlation (DIC) measurement technique was used to monitor displacements and cracks across the wall's surface.

**Preparation.** The laboratory-based production of TRM-reinforced rammed earth samples should reflect the on-site construction technique of rammed earth walls for test results to be meaningful and transposable. For this reason, a manual hand rammer was employed and the specimens had a minimum size (550x550x200 mm) so that size effects could be excluded.

The mixture was prepared considering the geotechnical analysis discussed in the previous section. The mixture was manually rammed into a wooden formwork (fig. 8a). The wallet consisted of nine layers, having thickness of about 61 mm each after compaction.

After a drying period of 28 days, the TRM was applied on both the surfaces of the rammed earth walls. A first layer was applied roughly to the wall (fig. 8b). Subsequently, the textile mesh was impregnated in the mortar setting the principal direction of the mesh perpendicular to the direction of the layers (fig. 8c). Finally, a second layer of mortar was applied (fig. 8c). After the application of the TRM, the specimens were stored to cure for a period of 28 days in laboratory conditions.



**Figure 8:** (a) Casting of RE wallet; (b) First layer of earth-based mortar; (c) Embedding of the mesh

**Set-up.** The diagonal compression test is used to study deformations of the wall that is loaded on one of its diagonals. Besides information about the different response phases and the failure mode, visual observation renders information about the origin and evolution of cracks. Before the specimen is put into the test set-up, it is painted white on both sides. In this way the development of the cracks throughout the test are easier to observe. After the drying process, one side is again painted, this time with black and white spray cans. The black and white dots render a fine speckle pattern on the surface which the DIC software needs to correlate images throughout the test to quantify deformations of the specimen.

The specimen was set diagonally on a steel support. Special care was taken to ensure a uniform contact and perfect alignment of the specimen with the displacement of the actuator. The displacements were recorded by two LVTDs set along the horizontal and vertical diagonal of one surface of the wallet (fig. 9a). Further digital image correlation (DIC) was implemented on the free surface. The stochastic pattern was created with black spots on white background and the frames were taken each 10 seconds (fig. 9b).

**Results.** The density of the rammed earth walls ( $\rho_{RE}$ ), water content (WC%), maximum shear stress ( $S_S$ ), maximum shear strain ( $\gamma$ ) and shear modulus ( $G$ ) are reported in table 1.

The average shear strength of the unreinforced walls (URE) is around 0,08 MPa. An improvement of the average found for the strengthened walls, namely 0,10 MPa for GRE and 0,09 MPa for the NRE. Silva (2013) reported an average maximum shear strength of 0,15 MPa for unreinforced walls compacted with a pneumatic hammer, resulting in a higher density and compaction.

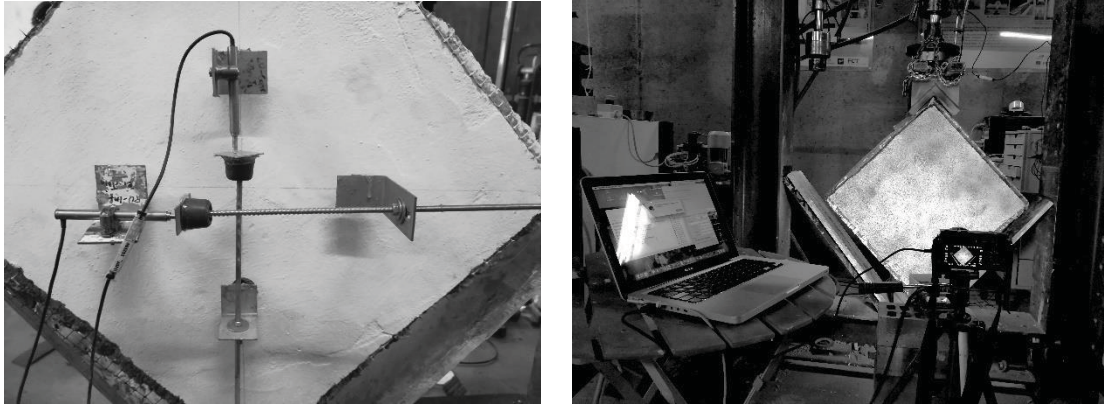


**Figure 9:** (a) Set-up of the diagonal compression test; (b) DIC equipment

The same trend is visible for the shear strain  $\gamma$  and shear modulus  $G$ . A decrease of 40% and 50% is found comparing the maximum shear strain of the unstrengthened wall with the ones calculated for glass fibre and nylon strengthened walls, respectively. Due to the reinforcement, the walls seem less easily deformed. The results for the shear modulus are less clear. On average higher  $G$  is found for the URE. However, these differences all lay within the standard deviation. Due to a faulty measure in the vertical LVDT, the  $G$  modulus could not be calculated for NRE2. Silva (2013) reports a shear modulus of 570 MPa and 709 MPa for URE-walls. As noted above, these higher values are to be expected given the different compaction parameters during construction.

Figure 10 shows the shear stress-strain curves of the walls. Due to non-coherent measurements of the LVDTs, some of the curves are cut reporting the reliable data.

In case of URE walls, after an elastic response characterized by the cohesion of the clay fraction, the peak stress is achieved as result from interlocking and friction of the larger particles. Sometimes a second peak is registered. This is attributed to a more severe interlocking of the larger particles. After the peak load, a large plateau is visible.

In case of strengthened rammed earth, the shear modulus is lower and the shear strength is reached for a much larger strain. Thus, the TRM improves the deformation capacity of the rammed earth. A bigger displacement is now allowed before failure. Not only does this influence the pre-peak behaviour of rammed earth, it also has an effect on what happens after the peak stress load. After peak load, the wall does not only have to rely on the internal contribution, but also on the stress-tensing of the TRM. The different reactions of the nylon and glass fibre are discussed in the next section.

Table 2 depicts the failure surfaces and failure modes of three samples of the tested walls that are representative for each of the wall types. Further comments are provided on visual inspections of the cracks. Similar cracks propagate throughout the wall irrespective of the reinforcement. A diagonal crack, through the different layers, occurs along the same direction of the applied load. When the load on the wall becomes too large, internal forces are not able to contain the failure of the element. The wall is broken into two pieces. This crack and failure mode is visible in all walls and is to be expected, as the test is designed to assess the shear behaviour with diagonal shear cracking as result. Sliding failure between the layers was feared. However, the bond between the layers proved to be sufficiently strong and not a dominant factor in the failure modes.

Following characteristics are observed only in the TRM-reinforced walls. First, instead of a complete failure and split into two parts, the textile holds the two parts of the wall together after the crack, proving the value of the system. Not only does the system make the wall less brittle, it also prevents it from failing completely. This can be a crucial feature during earthquakes. However, this theory should first be proven in field conditions.



**Table 1:** Results of diagonal compression test**(a) Results URE**

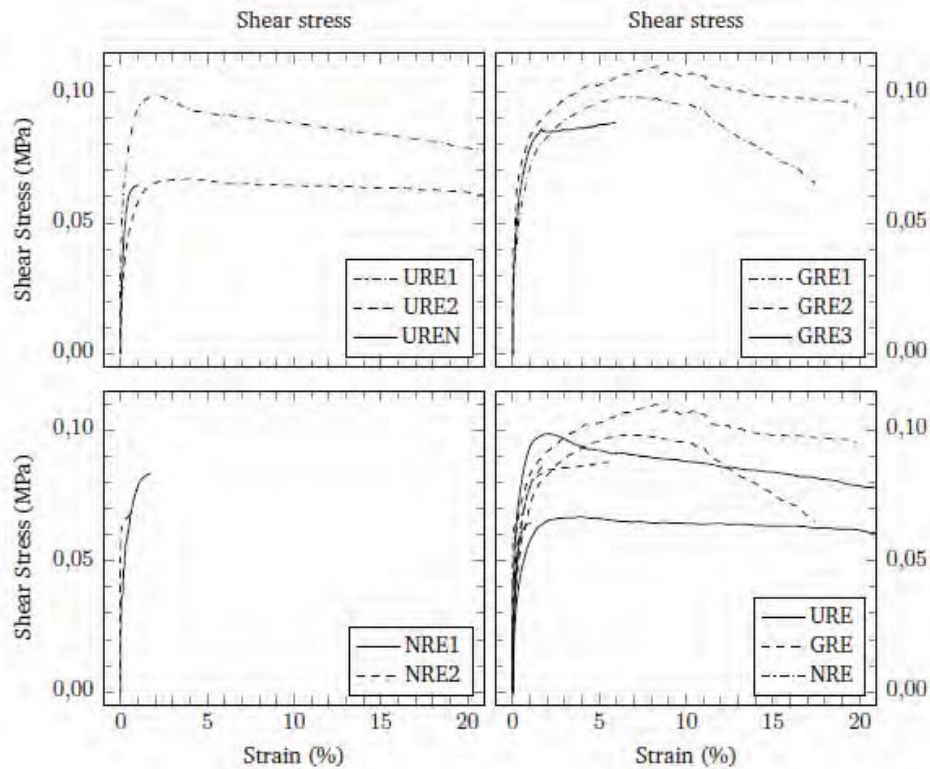
Wallet		URE1	URE2	UREN	Mean
wc	(%)	8,61	9,49	10,38	9,5±0,9
$\rho_{d,RE}$	(g/cm <sup>3</sup> )	2,13	2,15	2,02	2,1±0,07
$S_{S,max}$	(MPa)	0,10	0,07	0,08	0,08±0,02
$\gamma$	(-)	0,12	0,12	0,07	0,10±0,03
G	(MPa)	380	131	212	241±127

**(b) Results GRE**

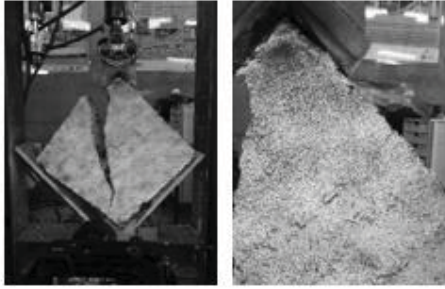
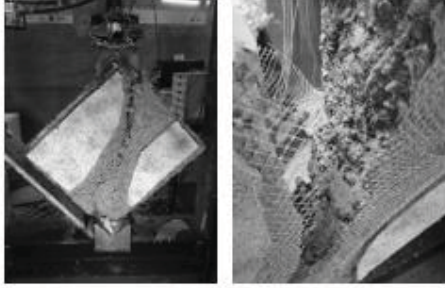
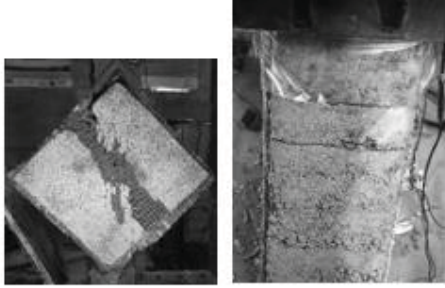
Wallet		GRE1	GRE2	GRE3	Mean
wc	(%)	9,51	8,47	9,52	9,2±0,96
$\rho_{d,RE}$	(g/cm <sup>3</sup> )	2,08	2,08	2,14	2,1±0,03
$S_{S,max}$	(MPa)	0,10	0,11	0,09	0,10±0,01
$\gamma$	(-)	0,06	0,09	0,02	0,06±0,03
G	(MPa)	99	162	198	153±50

**(c) Results NRE**

Wallet		NRE1	NRE2	Mean
wc	(%)	9,60	9,63	9,62±0,02
$\rho_{d,RE}$	(g/cm <sup>3</sup> )	2,11	2,14	2,13±0,02
$S_{S,max}$	(MPa)	0,094	0,082	0,088±0,008
$\gamma$	(-)	0,04	0,06	0,05±0,02
G	(MPa)	154	-	154±50

**Figure 10:** Shear stress - shear strain curves for a) unstrengthened walls (URE); b) strengthened walls with glass fibre based TRM (GRE) and c) walls strengthened with nylon based TRM (NRE).

**Table 2:** Failure modes of 3 of the tested specimens

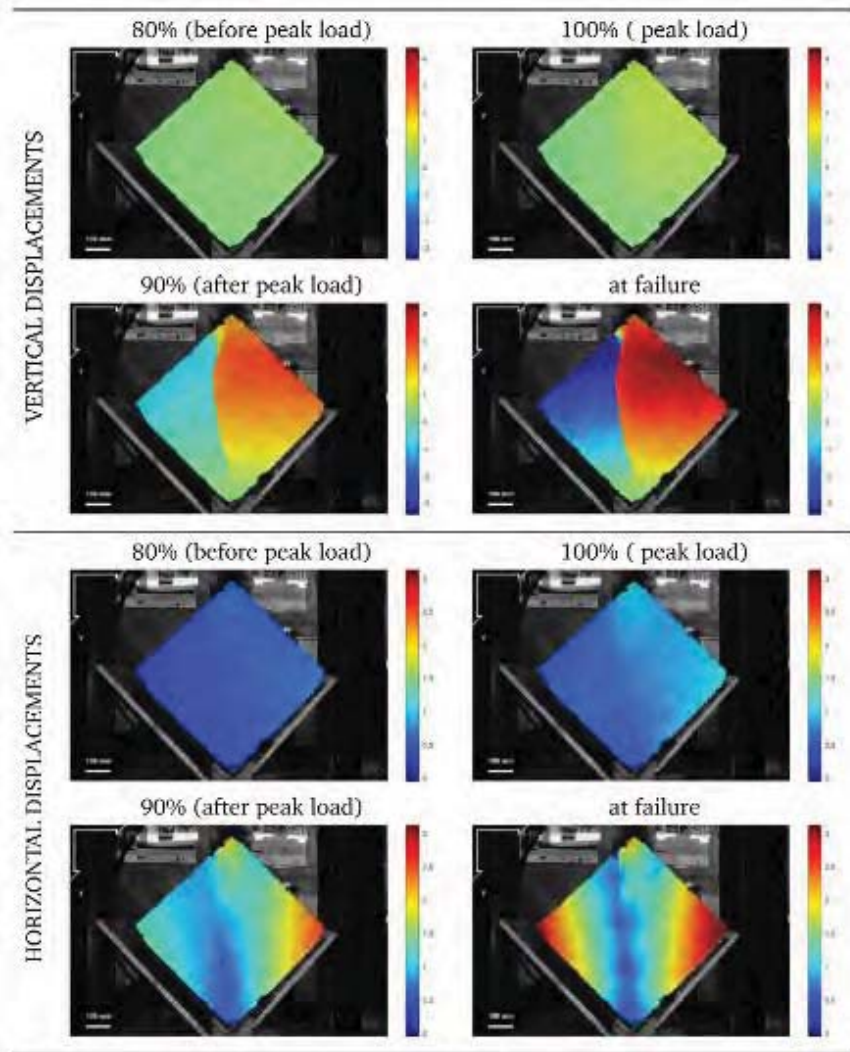
Wall	Failure mode	G	Comments
URE2		131	Main failure crack across all layers in direction of applied load. Cracks visible along main diagonal, side corners do not participate. Friction forces cause destruction of specimen. Shear cracks between layers visible after peak load.
GRE1		99	Main failure crack across all layers in direction of applied load. Crack pattern scattered. Friction forces cause destruction of specimen. Shear cracks between layers visible after peak load. TRM holds two halves together, also after completion of crack. Mortar detached.
NRE2		-	Main failure crack across all layers in direction of applied load. Crack pattern very scattered. Better distribution. Friction forces cause destruction of specimen. Multiple bigger shear cracks between layers visible after peak load. TRM holds two halves together, also after crack completion. Mortar detached parallel to main crack.

After the peak shear strength has been reached, smaller cracks between the interface of the layers start to propagate. These cracks start from the edges and make way towards the middle. The interface between layers are known to be weak spots when the wall is subjected to tension, as is the case on the sides during testing. However, the cracks have little to do with the ultimate failure.

Further smaller cracks are visible next to the primary diagonal crack. They propagate in a way similar to the primary crack. The differences between the different walls are clearer here. While the secondary cracks are not present in case of the URE walls, they do disperse much more on the reinforced walls. This is due to the effect of the TRM-system, in particular in case of NRE specimens. In the URE-case, the main diagonal is subjected to most of the load-bearing. Thus, the load is barely passed on to the sides of the specimen. This is not the case for the reinforced walls where the TRM-system activates the entire surface of the wall, causing multiple cracks over the entire surface.

Tables 3, 4 and 5 show the crack patterns that were observed by means of digital image correlation for each wall at 80%, 90% and 100% of the maximum force. All displacements are in reference to the positions in the original picture. The formation of the main cracks starts in a similar way for every wall. As an increasing load is applied along the main diagonal of the wall, compression starts to occur. This results in a slightly downwards displacement of the top particles, clearly visible at 80% of the maximum load.

**Table 3:** DIC visualisation results for wall URE2



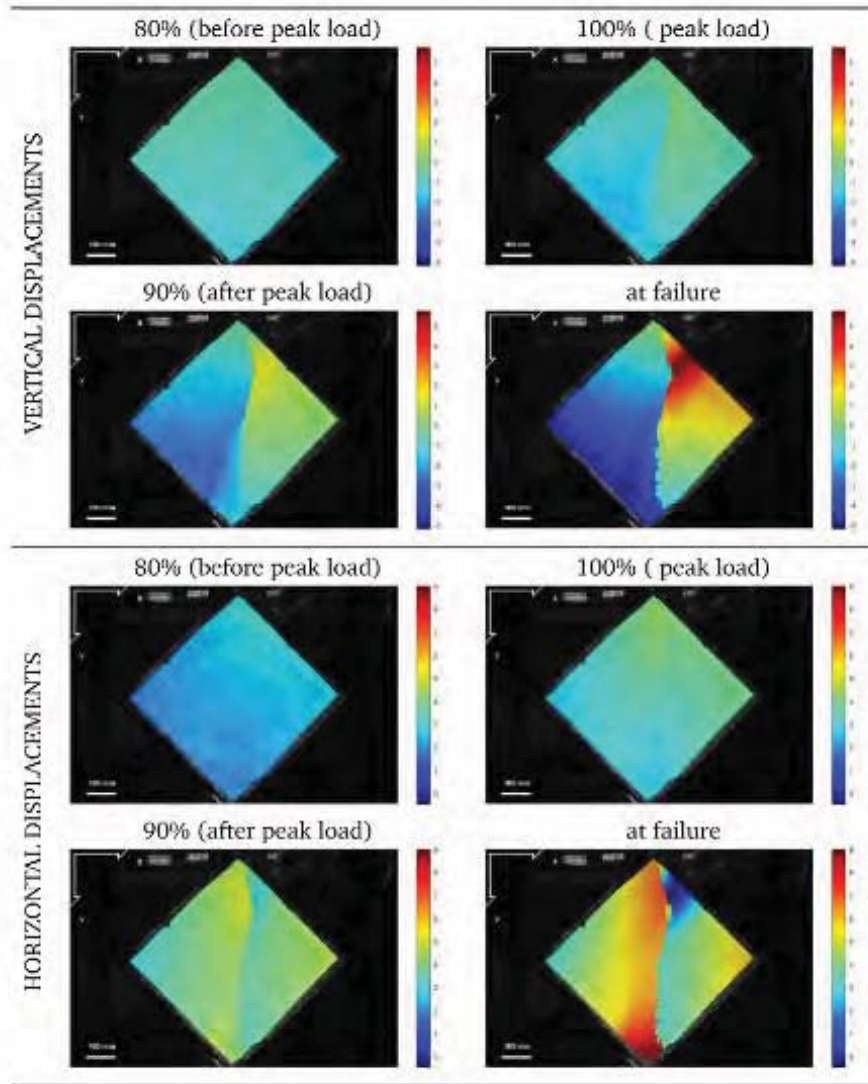
This compression gets more and more visible, as the load gets closer to the maximum peak load. At maximum peak load, the first signs of an eventual main crack become evident. This is definitely visible for the horizontal displacement. Left and right of the main diagonal, the particles start to move in the opposite direction, creating a crack. This horizontal outward displacement happens due to the compression of the particles in the vertical direction. It starts in the very middle of the wall and propagates along the horizontal diagonal; first to the top part of the wall, then to the bottom part. Even though the crack is not yet visible with the naked eye at peak load, it crosses the entire wall, developing to the edges next to the top and bottom support.

The main failure mode is similar for both the URE and RE walls. However, there are two differences. First of all, as stated previously, the TRM reduces the brittle behaviour of the wall, causing the peak load to occur at a later stage. This is clear in fig. 10. Secondly, the displacement and shear strain at peak load (as well as during the other loads) is higher for the reinforced than for the unreinforced walls, meaning that the TRM allows an improved non-elastic response of the wall.

After the peak load has been reached, larger differences between the URE and RE walls start to occur. As the wall is now completely cracked, the two parts of the wall start to behave independently. Due to the crack, the displacement around the crack remains 0 in the vertical direction for the URE walls.



**Table 4:** DIC visualisation results for wall GRE1

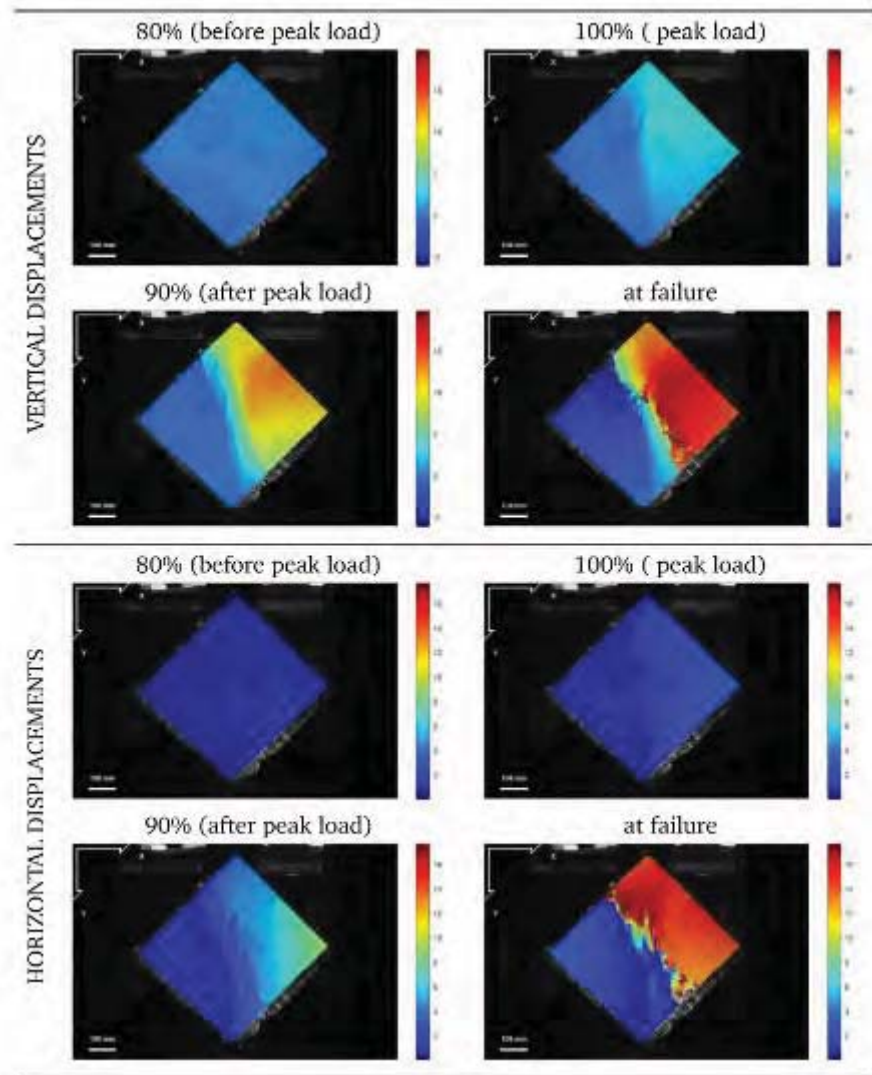


However, large displacements take place in the horizontal direction. This behaviour is different for the RE walls. As the TRM tries to avoid the crack from propagating, the particles get activated immediately around the crack. This influences the displacements in both the vertical and horizontal direction. In the horizontal direction the displacement gets opposed by the TRM, resulting in smaller displacements not only in relative value, but also in severity. At 90% of the maximum load in the decreasing branch, the maximum displacement already gets reached in the middle of the URE walls. This is not so for the TRM-strengthened walls. In the vertical direction, a more uniform displacement is found, in contrast with the behaviour of the URM-walls.

For some walls, the delamination at the interfaces between the layers becomes visible at 90% of the maximum load. This only happens after the peak load has been reached, confirming the conclusions drawn while testing. The largest horizontal displacements normally happen at this stage. Note however, that these cracks are formed in a way different from the main crack. Instead of two particles traveling in a different direction, here only the size of the displacement between two particles changes, not the direction. These cracks only propagate under these horizontal displacements, as no vertical displacements occur.



**Table 5:** DIC visualisation results for wall NRE2



Lastly, a comparison has been made between the NRE and GRE specimens. As previously observed, the TRM-system in general has a positive outcome on the displacement, brittleness and failure mode of rammed earth walls. Instead of a sudden failure, a more gradually deterioration is observed. Still, there exists also some textile-specific behaviour.

The shear modulus  $G$  shows almost no difference between the NRE and GRE mortars. One can conclude that there is little difference in rigidity and stiffness of the total structure. A similar result is found for the shear strain. The maximum shear strain seems higher in the GRE walls, but all differences are within standard deviation.

A different situation is observed for the cracks and failure modes of the reinforced walls. While the NRE walls have a more spread-out crack pattern, the cracks at the GRE walls are more concentrated in the centre area of the wall. Not only does the pattern itself changes, also the width and length of the cracks are different. While the cracks appear to be smaller, but higher in number for the NRE, they are bigger and fewer for the GRE. This phenomenon shows that there indeed is a difference in the distribution of the forces. It suggests that the nylon mesh helps to better distribute the forces to the sides of the wall, resulting in a more active behaviour of the entire wall. The opposite could be in effect for the glass fibre meshes. As the cracks in the centre part of the wall grow, the development of the distribution of the forces is stopped.

When looking at the final failure modes, this theory is confirmed. While the NRE walls have only a slight detachment of the mortar, this phenomenon is much more present for the GRE

walls. Important to point out here is the location where the detachment takes place. For both types of reinforced walls this happens between the mortar interface and the textile. Two conclusions can be made from this: 1. The bond between the mortar and the rammed earth substrate is sufficient. Not once did the strengthening system detach from the substrate; 2. The displacements in the rammed earth are not the direct reason for the detachment of the mortar, as far less cracks are visible on this inner mortar layer.

The resulting cracks seen on the surface are propagated due to the forces set on the matrix. These forces are passed on from the displacement of the rammed earth and mortar due to the load set on the rammed earth. As the mortar and rammed earth are both compressible, cracks are not formed yet in the beginning. However, due to these forces, the matrix is pulled into a stretched state, weakening the bond between the mortar and the matrix, resulting in the detachment of the mortar layer. As glass fibre is the stiffer material, this phenomenon will take place on a bigger scale. For nylon this is only localized. Even though the TRM reduces the brittleness of the rammed earth, as shown before, it does not prevent the failure mode of the rammed earth to occur. The layer of mortar between the textile and the rammed earth will behave similar to the rammed earth. The main crack will propagate through the rammed earth, starting from the top, retaining the mortar from distributing the forces through the entire wall.

#### **4. Conclusions**

This paper addresses the topic of the strengthening of rammed earth constructions by means of a textile reinforced mortar. Eight rammed earth walls were produced and strengthened to test their in-plane behaviour by means of a diagonal compression test. In so, knowledge could be developed regarding TRM as a strengthening technique.

Firstly, a geotechnical analysis was conducted on the soil. This knowledge was used to engineer the soil and make it more suitable for the rammed earth technique.

After the investigation of the characteristics of the materials, the walls were manually compacted and tested. The results indicate that the use of TRM provides an improvement in the non-linear behaviour of the walls, while the average shear strength is enhanced up to 25%. Furthermore, the crack pattern highlighted the capacity of the TRM to spread the force after achieving the peak load, in particular in case of NRE.

Finally, a comparison was made between the two textiles. It can be concluded that the nylon mesh delivered slightly better results in terms of the compatibility with the substrate, than the glass fibre mesh. Due to the stiffness of the matrix, a more active surface was reached, resulting in a better distributions of the forces.

#### **5. Bibliography**

- [1] Aaberg-Jorgenson, J. (2000). Clan Homes in Fuijan. *Arkitekten*, 28, 2-9.
- [2] ASTM (2003). ASTM E 519 – 02: Standard Test Method for Diagonal Tension (Shear) in Masonry Assemblages. American Society for Testing and Materials, West-Conshohocken, PA, United States of America.
- [3] Barroso, C.A. (2017). Reforço Sísmico Inovador de Construção de Taipa. MSc Thesis, Universidade do Minho, Guimarães, Portugal (in Portuguese).
- [4] Bernat-Maso, E. (2013). Analysis of unreinforced and TRM-strengthened brick masonry walls subjected to eccentric axial load. PhD Thesis, Universitat Politècnica de Catalunya, Barcelona, Spain.
- [5] Bui, Q.B. et al. (2009). Durability of rammed earth walls exposed for 20 years to natural weathering. *Building and Environment*, 44(5), 912-919.
- [6] Calderini, C., Cattari, S. & Lagomarsino, S. (2010). The use of the diagonal compression test to identify the shear mechanical parameters of masonry. *Construction and Building Materials*, 24(5), 677-685.

- [7] De Santis, S. & De Felice, G. (2015). Tensile behaviour of mortar-based composites for externally bonded reinforcement systems. *Composites Part B*, 68, 401-413.
- [8] Fuller, W.B. & Thompson, S.E. (1907). The Laws of Proportioning Concrete. *Transactions of the American Society of Civil Engineers*, 67-143.
- [9] Gomes, M. I., Gonçalves, T. D. & Faria, P. (2013). The compatibility of earth-based repair mortars with rammed earth substrates. 3<sup>rd</sup> Historic Mortars Conference, Glasgow, Scotland.
- [10] Houben, H. & Guillaud, H. (1989). *Earth construction: A comprehensive guide*. Intermediate Technology Publications, London, United Kingdom.
- [11] Jaquin, P.A. (2012). Influence of Arabic and Chinese Rammed Earth Techniques in the Himalayan Region. *Sustainability* 4, 2650-2660.
- [12] Jaquin, P.A., Augarde, C.E. and Gerrard, C.M. (2008). Chronological Description of the Spatial Development of Rammed Earth Techniques. *International Journal of Architectural Heritage*, 2(4), 377-400.
- [13] Lautrin, D. (1989). Utilization pratique des paramètres dérivés de l'essai au bleu de méthylène dans le projets de génie civil. *Bulletin des Liaison des Laboratoires des Ponts et Chaussées*, 160, 29-41.
- [14] Minke, G. (2006). *Building with earth: Design and technology of a sustainable architecture*. Birkhäuser Publishers for Architecture, Basel-Berlin-Boston.
- [15] Oliveira, D. et al (2017). Characterization of a Compatible Low Cost Strengthening Solution Based on the TRM Technique for Rammed Earth. *Key Engineering Materials*, 747, 150-157. DOI: 10.4028/www.scientific.net/KEM.747.150.
- [16] Pacheco-Torgal, F. & Jalali, S. (2012). Earth construction: Lessons from the past for future eco-efficient construction. *Construction and Building Materials*, 29, 512-519.
- [17] Papanicolaou, C., et al. (2007). Textile-reinforced mortar (TRM) versus FRP as strengthening material of URM walls: In-plane cyclic loading. *Materials and Structures*, 40(10), 1081-1097.
- [18] Silva, R. (2013). *Repair of Earth Constructions by Means of Grout Injection*. PhD thesis, Universidade do Minho, Departamento de Engenharia Civil, Guimarães, Portugal.
- [19] Van Gorp, M. (2018). *Experimental Study of the In-plane Behaviour of Rammed Earth, Strengthened with TRM*. MSc Thesis, KU Leuven.
- [20] Velde, B. (2008). Clay Minerals. *Terra Literature Review – An Overview of research in earthen architecture conservation*, 1-7.
- [21] Venkatarama, R. & Prasanna, K. (2010). Embodied energy in cement stabilised rammed earth walls. *Energy & Buildings*, 42(3), 380-385.
- [22] Warren, J. (1999). *Conservation of Earth Structures*. Butterworth-Heinemann, Oxford, United Kingdom.